Available online at www.sciencedirect.com

ScienceDirect

Procedia CIRP 117 (2023) 193–198

www.elsevier.com/locate/procedia

19th CIRP Conference on Modeling of Machining Operations

Model based design of tuned mass dampers for boring bars of small diameter

Wolfgang Hintze[a], Marco Hinrichs*[a], Oliver Rosenthal[a], Uwe Schleinkofer[b], Remus Venturini[b]

[a]*Hamburg University of Technology (TUHH), Institute of Production Management and Technology, Denickestrasse 17, 21073 Hamburg, Germany*
[b]*CERATIZIT Austria GmbH, Metallwerk-Plansee-Strasse 71, 6600 Reutte, Austria*

* Corresponding author. Tel.: +49-40-42878-3678 *E-mail address:* marco.hinrichs@tuhh.de

Abstract

Tuned mass dampers (TMD) are an established method to reduce self-excited chatter vibrations in turning. Regarding boring bars, the susceptibility to chatter increases with increasing length and, even more, with decreasing tool diameter.

A novel TMD for boring bars with diameters down to 10 mm is presented. The TMD-design, consisting of a mass and a spring-damper combination, is based on analytical and numerical modelling. By using a fluted boring bar design, the available design space allows to place a damping mass of sufficient mass ratio at the tool tip. Cutting tests showed the reduction of vibrations.

Keywords: Chatter; Boring; Damped boring bar; Damping; Tuned mass damper; Self-excited vibration; Modelling

1. Introduction

Tuned mass dampers are a well-established approach to reduce vibrations in machining operations using slender turning tools. In most cases, the occurring chatter vibrations are caused by self-excitation. These vibrations limit the maximum material removal rate of the cutting tool and cause poor surface quality as well as increased tool wear and noise. Research regarding chatter vibrations has identified various causes as well as concepts to avoid these. The tendency of a tool to chatter during the machining process is foremost defined by the frequency response function (FRF) of the tool, which represents the frequency-dependent compliance of a structure. [1, 2, 3] TMDs have been implemented successfully, also in industrial applications, in order to improve the dynamic behaviour of boring bars [4]. The underlying concept uses an additional damped spring-mass system, which is attached to an existing structure. Given the parameters of the TMD being tuned optimally, the configuration will reduce the resonance magnification of the original structure significantly. In case of boring bars, this is usually the first bending mode.

Nomenclature

A_{RMS}	Root mean square of amplitudes
c_i	(Modal) damping
D	Diameter of boring bar
d	Diameter of damping mass
f_i	Eigenfrequency i
f_{DH}	Frequency ratio of TMD mass and tool modal mass
k_i	(Modal) stiffness
k_{SD}	Stiffness of single SD-element
L	Length or overhang of boring bar
m_i	(Modal) mass i
μ	Mass ratio m_2/m_1

Concepts and mechanisms using actively damped or self-tuning TMD to overcome this issue are part of a wide field of research showing a high level of activity. Important contributions during recent years are summarised below. The current research can be clustered into two main groups: Development of TMD designs (subdivided into active and passive damping mechanisms) and modelling approaches to predict process behaviour as well as methods for tuning (newly developed or already existing) designs in order to achieve optimised process damping.

10.1016/j.procir.2023.03.034

Matsubara stated in 2014 *"Tuned mass dampers (TMDs) are classical passive vibration absorbers, for which the tuning process was established by Den Hartog"* [5]. Hendrowati et al. designed a thin steel tube surrounding the boring bar near the cutting edge and supported by rubber rings as a passive TMD (D = 25 mm, L = 200 mm) [6]. Hayati et al. proposed a frictional damping concept with longitudinal pressfitted pins inside the bar to dissipate energy under bending vibrations and demonstrated the successful performance for a boring bar (D = 25mm, L = 180 mm) [7]. Chockalingam et al. used a mix of copper and zinc particles located in cavities inside the tool to reduce the vibrations of a boring bar (D = 25 mm, L = 200 mm) [8]. Vogel et al. showed the damping capability of a similar concept using specially structured and particle-filled hollow elements in an external tuning tool when machining titanium [9]. Fu et al. covered the clamping interface of a boring bar by using a carbon nanocomposite damping coating and achieved a reduction of noise and surface roughness in machining tests (D = 25 mm, L = 125 mm) [10]. Liu et al. developed a TMD with variable stiffness (D = 40 mm, L = 600 mm) [11]. Matsubara et al. showed, that a piezoelectric actuator integrated into a boring bar and connected to a LR-circuit can act similarly to a TMD. The authors demonstrated the improved performance by measuring the displacement in cutting tests (D = 16 mm, L = 120 mm) [5]. Chen, Lu et al. used an actively controlled magnetic actuator to enhance the process stability of a boring bar regarding chatter vibrations (D = 25 mm, L = 305 mm) [4].Sørby and Østling attached strain gauges for tool deflection measurement to a TMD-equipped boring bar in order to increase machining precision by deflection-based machining strategies (D = 60 mm, L = 600 mm) [12].

Bansal and Law described a receptance coupling approach to tune a TMD attached to a boring bar. The modelling is based on an Euler-Bernoulli beam and is applied to a tool with diameter D = 25 mm and L = 300 mm overhang [13]. Fallah and Moetakef-Imani predicted the boundaries of process stability for a TMD-equipped boring bar (D = 47 mm, L = 720 mm) [14]. Yuhuan et al. developed a theoretical model to calculate the performance of a composite boring bar with multiple layers of material to benefit from constrained layer damping (D = 32 mm, L = 500 mm) [15].

Østling and Magneval used a combination of bending vibration of the boring bar and rotational vibration of the clamping strucure for modelling the dynamic behaviour of a large boring bar (D = 200 mm, L = 1521 − 2118 mm) [16]. When investigating the dynamic behaviour of TMDs with constrained movement, Iklodi et al. found, that mass collisions between the damping mass and a wall could decrease damping and therefore should be avoided [17].

Lawrance et al. also provide a comprehensive review of chatter suppression in boring operations [18].

Looking at the research regarding dynamic stability and tuned mass dampers conducted up to now reveals, that all studies were performed using tools of diameters $D \geq 16$mm or even $D \geq 25$ mm, which makes the implementation of TMDs easier due to the available design space. However, for many industrial applications, boring bars of smaller diameters D and overhangs L are used. Therefore, the issue of enhancing dynamic stability by using suitable TMDs is highly relevant for smaller tools.

This paper describes the concept, dimensioning and performance trials of a tuned mass damper exemplarily for two boring bars in the field of small diameters and overhangs, see Figure 1. Fundamental dimensioning of the investigated TMDs is done using an analytical method and is subsequently optimised by means of FEM in order to minimise the absolute negative real part of the receptance in the frequency response function, which is most crucial for the occurrence of regenerative chatter [2]. The manufactured TMDs are implemented into prototype tools, whose performance in turning tests is compared to reference tools without TMD. The process stability during turning tests is evaluated using structure-borne sound emissions resulting from the machining process and the obtained surface quality.

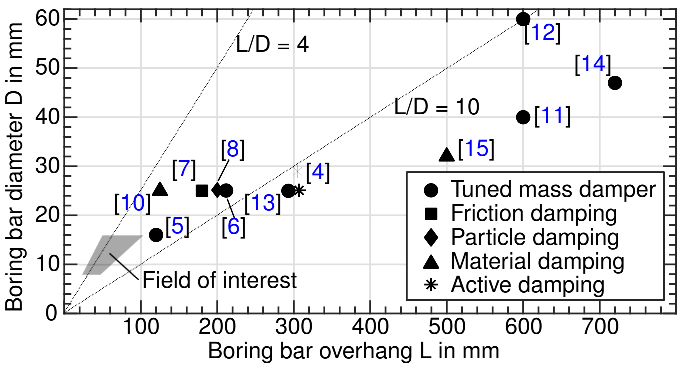

Fig. 1. Research regarding damped boring bars, arranged by diameter, overhang and damping mechanism.

2. Boring bar and TMD Design

To investigate the damping potential of tuned mass dampers for different dimensions, prototype TMDs for two tools based on *Ceratizit EcoCut* boring bars with diameter D = 16 mm and D = 10 mm as well as overhang-to-diameter ratios of L/D = 4 are designed and implemented into the tools. Main application of the boring bars are internal longitudinal turning operations. Therefore, the tool stiffness in feed direction is very high and thus is considered as ideal stiff, whereas the lower stiffness perpendicular to the longitudinal tool axis in combination with radial forces is responsible for the chatter vibrations, which should be suppressed [19]. The *EcoCut* boring bar is characterised by a specific cross section of an approximate three-quarter circle providing design space for positioning the TMD next to the cutting insert at the tool tip. Thereby, the overall tool stiffness stays almost unaffected. Moreover, as the dynamic deflections are highest at the tool tip, a TMD positioned here is assumed to be most effective. The tuned mass damper consists of a mass, which is located between two polymer layers, the latter hereinafter referred to as spring-damper (SD-)elements. The TMD is placed in a corresponding cavity near the tip of the boring bar. In order to guarantee easy manufacturing and to ensure a uniform transmission of forces along the complete contact surface between damping mass and SD-elements, the latter are made of adhesive. The boring bars allow the placement of the damping unit inside a fully closed cavity drilled into the front face of the tool. This provides most effective protection against chips and cooling lubricant. The adhesive used for both TMDs has a shear modulus of $G = 250$ MPa at room temperature.

The different TMD designs for both diameters is shown in Figure 2. According tools without TMD were investigated for comparison purposes.

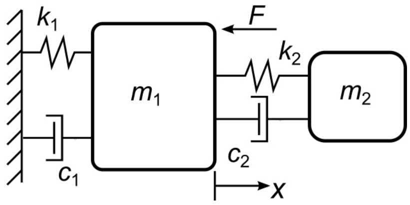

Fig. 3. Model of a TMD with two degrees of freedom.

3. Analytic modelling of tuned mass damper

Figure 3 shows the simplified analytical model of a tuned mass damper with two degrees of freedom (DOF). The optimal frequency ratio f_{DH} of a TMD located at the tool tip is given by equations developed by Hartog [20] and Sims [21]. The effective attachment point of the TMDs is assumed to be in the center of the mass and is around $f_{DH} = 0.7L$. According to Bansal, the optimal frequency ratio can be estimated to $f_{DH,16} = 0.97$ for the boring bar with $D = 16$ mm respectively to $f_{DH,10} = 1.0$ for the one with $D = 10$ mm [13]. Given this frequency ratio, the required stiffness of the TMD is calculated using equation (4).

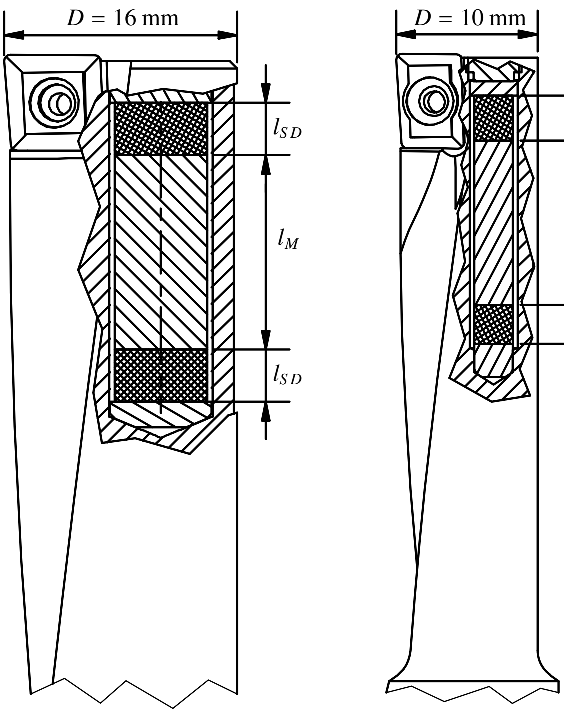

Fig. 2. Designs of TMDs for boring bars with diameter $D = 16$ mm and $D = 10$ mm. The relevant dimensions are the lengths of the spring-damper elements (l_{SD}) and of the mass (l_M). The prototype boring bars consist of a TMD in a fully-closed cavity.

$$F = m_1\ddot{x} + c_1\dot{x} + k_1 x \tag{1}$$

$$f_{DH} = \frac{f_2}{f_1} \tag{2}$$

$$\mu = \frac{m_2}{m_1} \tag{3}$$

$$f_i = \frac{1}{2\pi}\sqrt{\frac{k_i}{m_i}} \Rightarrow k_i = m_i(2\pi f_i)^2 \qquad i = 1, 2 \tag{4}$$

Mass m_1, stiffness k_1 and damping factor c_1 of the first 1-DOF-system (1) are identified by peak picking based on a measured frequency response function of the unmodified reference tools as described by Schmitz [22]. The mass m_2 of the TMD is a design parameter, which is limited by the design space available. According to Munoa and Yang, a mass ratio of $\mu = 0.05$ can be sufficient to reduce chatter, whereas a ratio of $\mu = 0.2$ or higher is typical in industrial applications [2, 23]. With the given mass m_2 and mass ratio μ, the desired frequency f_2 and stiffness k_2 are calculated by using equations (2) and (4). The damping coefficient c_2 of the SD-elements only depends on material and geometrical parameters. An optimal value cannot be achieved due to conflicting requirements, whereby meeting the stiffness requirements has priority over the damping coefficient.

With a given cross section A (and according area moment of inertia I) of the SD-elements defined by the design space restrictions as shown in Figure 2, the desired stiffness k_2 is dependent on the length l_{SD} as well as the material parameters shear modulus G and Young's modulus E. When the mass is deflected perpendicular to the longitudinal boring bar axis, both spring-damper elements undergo a combination of shear and bending deformation. The required length of the SD-elements is calculated by taking the shear stiffness k_{shear} and the bending stiffness k_{bend} into account, see equations (5) snd (6). The bending stiffness k_{bend} is calculated based on Euler beam theory by assuming, that both contact surfaces of each SD-element stay parallel to each other as the deformations are small. For a cantilever beam with one end fixed and one end guided and a force applied to at the guided end, the bending stiffness is given by formula (6) [24]. Assuming, that both stiffnesses are independent of each other and act like two serial-connected springs, the resulting stiffness of one SD-element k_{SD} is given by (7). The length l_{SD} is calculated numerically or graphically by solving this equation.

$$k_{shear} = \frac{GA}{l_{SD}} \quad (5)$$

$$k_{bend} = \frac{12EI}{l_{SD}^3} \quad (6)$$

$$k_{SD} = \frac{k_2}{2} = \frac{k_{shear} \cdot k_{bend}}{k_{shear} + k_{bend}} = \frac{12GAI}{GAl_{SD}^3 + 12EI} \quad (7)$$

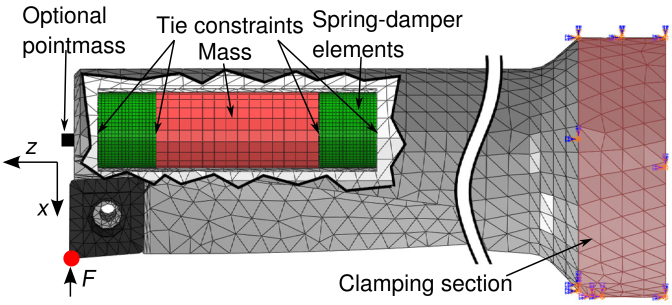

Fig. 4. Finite element model used to calculate frequency response functions of a TMD-equipped boring bar for the point of interest at the corner radius of the cutting insert. The TMD located in a cavity inside the tool is shown in a cutout. Tie constraints are used to connect the spring-damper-elements with the boring bar body and the mass. The optional point mass accounts for the mass of the acceleration sensor and is added to the model allowing comparison with measurements.

4. Finite element modelling

In order to assess and optimise the selected TMD designs with regard to their dynamic compliance, finite element models (FEM) are used to minimise the absolute negative real part of the according frequency response function, which serves as optimisation criterion. In contrast to the analytical model, the FEM does not assume the shear tension being equally distributed along the cross section of the SD-elements. Furthermore, in longitudinal direction of the TMD, both SD-elements undergo different dynamic displacements. The effective force attack point of the TMD on the tool axis is defined in the FEM by taking the axial distributions of mass, stiffness and damping into account. On the other hand, the FEM is not based upon a measurement and does not account for the overall stiffness of the machining system so far. The FRF was calculated for impacts in x-direction, corresponding to the direction of the passive force in the plane perpendicular to the tool axis using the so-called linear perturbation step of ABAQUS with the corner of the cutting edge being the point of impact and interest, see Figure 4. Tie constraints are used to connect the SD-elements with the boring bar body and the mass. The optional point mass accounts for the mass of the acceleration sensor and can be added to the model, thus allowing comparison with measurements. The clamping area of the boring bar was constrained rigidly (all degrees of freedom locked in ABAQUS). To evaluate different TMD dimensions and optimise the design, the SD-element length l_{SD} and mass length l_M is modified by a python program, which modifies the CAD model based on a predefined parameter list and initiates the FRF-calculation.

5. Experimental setup

In order to analyse the dynamic behaviour, the dynamic compliance of the boring bars was measured using modal hammer excitation. For all investigations, the excitation is performed in passive force direction, which aligns with the x-axis of the machine tool. It must be noted, that the measurement is subject to inaccuracies due to the sensor mass being in the same order as the modal mass, especially for the boring bar with D = 10 mm. For validation purposes, the performance of the damped and undamped boring bars was investigated in longitudinal turning tests on a CNC lathe. Steel 42CrMo4 (1.7225) was machined using cooling lubricant at a cutting speed of v_c = 200 m/min. Cutting depth and feed vary in a range of a_p = 0.1 – 0.8 mm respectively f = 0.07 – 0.13 mm. The minimum feed path of each test was l_f = 20 mm. All cutting inserts had a corner radius of r_ϵ = 0.4 mm. The process stability was measured by recording the process-induced structure-borne sound using a *Qass* piezoelectric measurement system. The transducer was mounted in a dry area on the turret.

The machined surfaces were photographed after each cut. Evaluation of the process stability is based on the root mean square A_{RMS} of the recorded signal after a low pass filter of 20 kHz has been applied.

For comparing the amplitude levels A_{RMS} between the individual cutting tests, the audio signal, calculated over a period of 1 second just prior to the initial tool contact with the workpiece, was taken as reference and used as scaling factor.

6. Results

The results cover the TMD design and experimental investigations for two representative tool diameters.

For the boring bar with D = 16 mm, the TMD design yields a diameter of d = 6.4 mm for the damping mass, respectively d = 2.8 mm for the D = 10 mm boring bar, each limited by the given design space. The resulting parameters and dimensions of the analytical and the FEM approach are listed in Table 1.

Table 1. Modal parameters obtained by peak picking, stiffness, mass parameters and dimensions of the tuned mass dampers.

D in mm	f_1 in Hz	m_1 in g	μ	f_{inDH}	k_2 in $\frac{N}{m}$	l_{SD} in mm	l_M in mm
Analytic approach							
10	2240	2.7	0.4	1.0	1.64E5	5	11
16	1724	11.8	0.64	0.97	8.21E5	7.6	14
FEM approach (realised)							
10	2550					3	11
16	1904					5	14

In addition to the fundamental analytical calculations, the FEM approach is used to analyse the effect of varying geometric design parameters on the dynamic compliance of the damped boring bar, which are hard to identify from the calculations alone. Based on the analytical calculations, refined by FEM, two prototypes with the dimensions given in Table 1 were manufactured.

To achieve a constant frequency ratio f_{DH}, a higher mass length l_M requires a higher stiffness k_2 and therefore shorter SD-elements, thus counteracting the higher mass length and keeping the overall length l of the TMD unit ($l = l_M + 2 \cdot l_{SD}$) within a limited range.

Measured and calculated FRFs of the TMD-equipped boring bars are compared to the undamped reference tools, see Figure 5. For both tool diameters, the amplitude magnification is significantly reduced, for measurement as well as FEM, and the curves show the characteristic profile of a TMD consisting of two peaks.

All tools were investigated in turning tests regarding their dynamic stability behaviour under different parameters. The tests show an increased process stability for the damped boring bars across nearly all parameters regarding the scaled amplitude of the structure-borne sound (Figure 6). This correlates with the machined workpiece surfaces quality, based on qualitative optical assessment and the acoustic noise level as well.

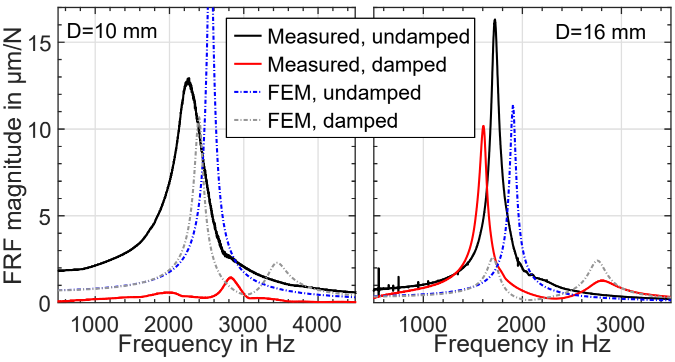

Fig. 5. Frequency response function of TMD-equipped and undamped boring bars. Comparision of measurement and FEM.

7. Discussion

The results of the design calculations based on analytical methods and those obtained by FEM lead to different results. The analytically calculated optimal thicknesses of the SD-elements are significantly higher than those derived by FEM. The main reasons for this are presumably the location of the TMD unit, which is approximated in the analytic model, the sensor mass and the removed material of the cavity, which is not considered in the analytical model. Furthermore, the deformation modelling of the SD-elements is simplified. An improved modelling of their bending and shear behaviour might be possible using Timoshenko beam theory. In addition, the SD-elements contribute to the overall system mass of the TMD, but

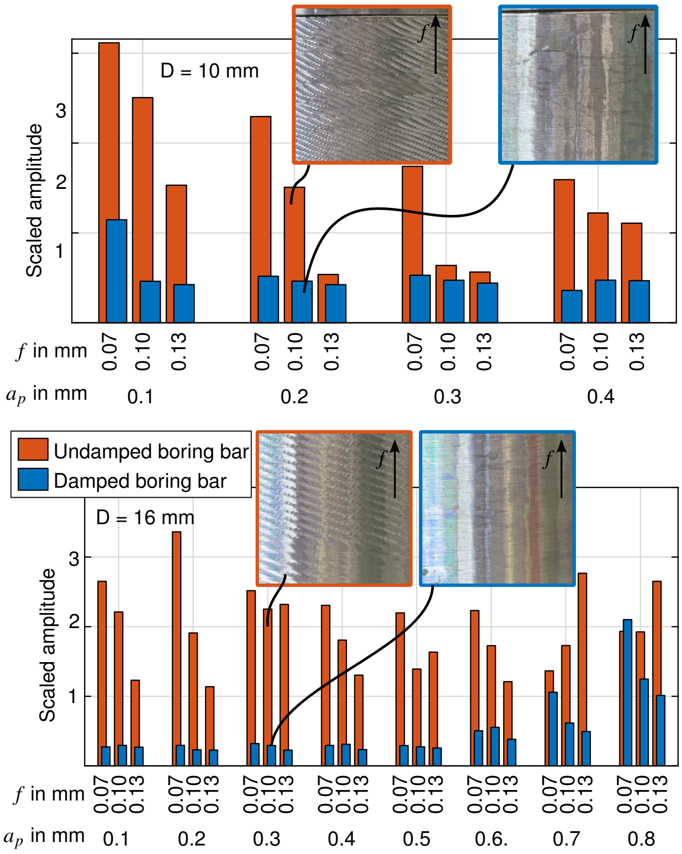

Fig. 6. Comparison of scaled structure-borne sound signals of undamped and TMD-equipped boring bars for different cutting parameters. Examples of resulting surface qualities are given.

are considered to have no mass in the analytical calculations so far.

When tuning smaller boring bars, special attention regarding precise manufacturing of the SD-elements is vital, since small deviations can have a high impact on k_{SD}.

In contrast to the analytical approach discussed above, the FEM, which is not based on measurements, allows to take the aforementioned complex SD-element deformation into account. On the other hand Figure 5 shows relevant deviations in the eigenfrequency wich are caused by certain simplifications and uncertainties and have to be accepted. A smaller boring bar diameter leads to higher deviations. The FEM does not account for the overall compliance of the machining system so far. Additionally, the exact overhang of the boring bars is unknown due to the clamping mechanism of the shaft-tool holder interface. Due to the clearance fit and the clamping screws, the effective free lenght of the boring bar might extend some millimeters inside the tool holder, thus representing a factor of uncertainty.

Due to the mass of the acceleration sensor (mass: $m_{acc} = 1$ g), to which the unknown effective mass of the attached cable (mass: $m_{cab} = 1 - 2$ g) contributes as well, the measured FRFs are affected. This is an additional cause for mismatch between measured and simulated FRFs, especially for the small tool diameter $D = 10$ mm with a modal mass of $m_1 = 2.7$ g. To compensate this effect, an additional pointmass (Figure 4) is used as an approximation.

Particularly for the diameter $D = 10$ mm, the chip removal energy transferred to the tool shaft and therefore the TMD unit, can lead to a significant temperature increase over cutting time, thus resulting in a stiffness reduction of the spring-damper material and to a final loss of dynamic stability. To overcome this issue, the test were conducted using cooling lubricant.

Despite the limitations of the described models and simulations, these methods turned out to provide valuable information for the design of tuned mass dampers for optimised boring bars. The amplitude magnification was significantly reduced and the process stability during cutting tests proved an enhanced performance of this damping concept for small diameters.

8. Conclusion

Machining operations using slender boring bars with long overhang and a high L/D-ratio lead to significant challenges regarding the dynamic process stability, today often limiting productivity and reliable part quality. Tuned mass dampers offer a high potential for process optimisation with respect to dynamic stability especially for finishing operations, where common chatter-avoiding strategies by adjusting the cutting parameters, mainly the depth of cut, are not applicable. The presented research has shown, that the concept of TMDs can be adapted to boring bars with diameters down to $D = 10$mm despite the limited design space. Validated by measured magnitude amplifications at the relevant eigenfrequencies, the dynamic compliances for TMD-equipped boring bars were significantly reduced. Related to this, the noise amplitudes in cutting tests were reduced significantly and the machined surface quality increased correspondingly. Thus, cutting tests clearly confirm the increased performance of the TMD-equipped boring bars. The benefit of detailed analytical modelling and FEM, especially when looking at slender tools and high eigenfrequencies became apparent.

9. Acknowledgments

The authors would like to thank Ceratizit Austria GmbH for funding the presented research.

References

[1] M. Siddhpura, R. Paurobally, A review of chatter vibration research in turning, International Journal of Machine Tools and Manufacture 61 (2012) 27–47. doi:10.1016/j.ijmachtools.2012.05.007.
[2] J. Munoa, X. Beudaert, Z. Dombovari, Y. Altintas, E. Budak, C. Brecher, G. Stepan, Chatter suppression techniques in metal cutting, CIRP Annals 65 (2) (2016) 785–808. doi:10.1016/j.cirp.2016.06.004.
[3] X. A. Vasanth, P. S. Paul, G. Lawrance, A. S. Varadarajan, Vibration control techniques during turning process: a review, Australian Journal of Mechanical Engineering 19 (2) (2021) 221–241. doi:10.1080/14484846.2019.1585224.
[4] F. Chen, M. Hanifzadegan, Y. Altintas, X. Lu, Active damping of boring bar vibration with a magnetic actuator, IEEE/ASME Transactions on Mechatronics 20 (6) (2015) 2783–2794. doi:10.1109/TMECH.2015.2393364.
[5] A. Matsubara, M. Maeda, I. Yamaji, Vibration suppression of boring bar by piezoelectric actuators and LR-circuit, CIRP Annals 63 (1) (2014) 373–376. doi:10.1016/j.cirp.2014.03.132.
[6] W. Hendrowati, N. Merdekawan, Modeling and analysis of boring bar vibration response in internal turning due to variation of the amount of dva rubber in finish boring cut, Journal of Mechanical Science and Technology 35 (10) (2021) 4353–4362. doi:10.1007/s12206-021-0907-3.
[7] S. Hayati, M. Shahrokhi, A. Hedayati, Development of a frictionally damped boring bar for chatter suppression in boring process, The International Journal of Advanced Manufacturing Technology 113 (9-10) (2021) 2761–2778. doi:10.1007/s00170-021-06791-3.
[8] S. Chockalingam, U. Natarajan, A. George Cyril, Damping investigation in boring bar using hybrid copper-zinc particles, Journal of Vibration and Control 23 (13) (2017) 2128–2134. doi:10.1177/1077546315610946.
[9] F. A. Vogel, S. Berger, E. Özkaya, D. Biermann, Vibration suppression in turning TiAl6V4 using additively manufactured tool holders with specially structured, particle filled hollow elements, Procedia Manufacturing 40 (2019) 32–37. doi:10.1016/j.promfg.2020.02.007.
[10] Q. Fu, D. Lundin, C. M. Nicolescu, Anti-vibration engineering in internal turning using a carbon nanocomposite damping coating produced by pecvd process, Journal of Materials Engineering and Performance 23 (2) (2014) 506–517. doi:10.1007/s11665-013-0781-y.
[11] X. Liu, Q. Liu, S. Wu, L. Liu, H. Gao, Research on the performance of damping boring bar with a variable stiffness dynamic vibration absorber, The International Journal of Advanced Manufacturing Technology 89 (9-12) (2017) 2893–2906. doi:10.1007/s00170-016-9612-2.
[12] K. Sørby, D. Østling, Precision turning with instrumented vibration-damped boring bars, Procedia CIRP 77 (2018) 666–669. doi:10.1016/j.procir.2018.08.181.
[13] A. Bansal, M. Law, A receptance coupling approach to optimally tune and place absorbers on boring bars for chatter suppression, Procedia CIRP 77 (2018) 167–170. doi:10.1016/j.procir.2018.08.267.
[14] M. Fallah, B. Moetakef-Imani, Analytical prediction of stability lobes for passively damped boring bars, Journal of Mechanics 33 (5) (2017) 641–654. doi:10.1017/jmech.2017.22.
[15] Z. Yuhuan, R. Yongsheng, T. jishuang, M. jingmin, Chatter stability of the constrained layer damping composite boring bar in cutting process, Journal of Vibration and Control 25 (16) (2019) 2204–2214. doi:10.1177/1077546319852240.
[16] D. Østling, M. Magnevall, Modelling the dynamics of a large damped boring bar in a lathe, Procedia CIRP 82 (2019) 285–289. doi:10.1016/j.procir.2019.04.041.
[17] Z. Iklodi, D. A. Barton, Z. Dombovari, Bi-stability induced by motion limiting constraints on boring bar tuned mass dampers, Journal of Sound and Vibration 517 (2022) 116538. doi:10.1016/j.jsv.2021.116538.
[18] G. Lawrance, P. Sam Paul, A. S. Varadarajan, X. Ajay Vasanth, S. B. Raj, Suppression of tool vibration in boring process: A review, Journal of The Institution of Engineers (India): Series C 100 (6) (2019) 1053–1069. doi:10.1007/s40032-019-00531-z.
[19] E. Budak, E. Ozlu, Analytical modeling of chatter stability in turning and boring operations: A multi-dimensional approach, CIRP Annals - Manufacturing Technology 56 (1) (2007) 401–404. doi:10.1016/j.cirp.2007.05.093.
[20] J. P. den Hartog, Mechanical vibrations, 4th Edition, McGraw-Hill Book Company Inc, New York and Toronto and London, 1956.
[21] N. D. Sims, Vibration absorbers for chatter suppression: A new analytical tuning methodology, Journal of Sound and Vibration 301 (3-5) (2007) 592–607. doi:10.1016/j.jsv.2006.10.020.
[22] T. L. Schmitz, K. S. Smith, Machining Dynamics, Springer International Publishing, Cham, 2019. doi:10.1007/978-3-319-93707-6.
[23] W. Ma, J. Yu, Y. Yang, Y. Wang, Optimization and tuning of passive tuned mass damper embedded in milling tool for chatter mitigation, Journal of Manufacturing and Materials Processing 5 (1) (2021) 2. doi:10.3390/jmmp5010002.
[24] W. C. Young, R. G. Budynas, W. C. Young, R. G. Budynas, R. J. Roark, Roark's Formulas for Stress and Strain, 7th Edition, McGraw-Hill, New York, NY, 2007.